microbial biotechnology

Open Access

Metabolic modulation of redox state confounds fish survival against *Vibrio alginolyticus* infection

Qi-yang Gong,[1,2] Man-jun Yang,[1] Li-fen Yang,[3] Zhuang-gui Chen,[3] Ming Jiang[1,2] and Bo Peng[1,2,3,4]*

[1]*State Key Laboratory of Bio-Control, Guangdong Key Laboratory of Pharmaceutical Functional Genes School of Life Sciences, Center for Proteomics and Metabolomics, Sun Yat-sen University, Guangzhou, 510006, China.*

[2]*Laboratory for Marine Biology and Biotechnology, Qingdao National Laboratory for Marine Science and Technology, Qingdao 266071, China.*

[3]*Department of Pediatrics, The Third Affiliated Hospital of Sun Yat-sen University, Guangzhou 510630, China.*

[4]*Southern Marine Science and Engineering Guangdong Laboratory (Zhuhai), Zhuhai 519000, China.*

Summary

Vibrio alginolyticus **threatens both humans and marine animals, but hosts respond to *V. alginolyticus* infection is not fully understood. Here, functional metabolomics was adopted to investigate the metabolic differences between the dying and surviving zebrafish upon *V. alginolyticus* infection. Tryptophan was identified as the most crucial metabolite, whose abundance was decreased in the dying group but increased in the survival group as compared to control group without infection. Concurrently, the dying zebrafish displayed excessive immune response and produced higher level of reactive oxygen species (ROS). Interestingly, exogenous tryptophan reverted dying rate through metabolome re-programming, thereby enhancing the survival from *V. alginolyticus* infection. It is preceded by the following mechanism: tryptophan fluxed into the glycolysis and tricarboxylic acid cycle (TCA cycle), promoted adenosine triphosphate (ATP) production and further increased the generation of NADPH. Meanwhile, tryptophan decreased NADPH oxidation. These together ameliorate ROS, key molecules in excessive immune response. This is further supported by the event that the inhibition of pyruvate metabolism and TCA cycle by inhibitors decreased *D. reiro* survival. Thus, our data indicate that tryptophan is a key metabolite for the host to fight against *V. alginolyticus* infection, representing an alternative strategy to treat bacterial infection in an antibiotic-independent way.**

Received 16 October, 2019; revised 18 January, 2020; accepted 23 February, 2020.
*For correspondence. E-mail pengb26@sysu.edu.cn; Tel. +86 20 8411 1708; Fax: +86 20 8403 6215.
Microbial Biotechnology (2020) **13**(3), 796–812
doi:10.1111/1751-7915.13553
Funding information
This work was sponsored by grants from NSFC project (31822058, 31672656, 31872602), and the Fundamental Research Funds for the Central Universities (18lgzd14, 19lgyjs42).

Introduction

Vibrio alginolyticus, a salt-tolerant Gram-negative bacterium commonly found in temperate marine and estuarine environments, causes human superficial wound and otitis (Di Pinto *et al*., 2005; Reilly *et al*., 2011). Meanwhile, *V. alginolyticus* is an important fish pathogen that is isolated as causative agent of vibriosis in cultured gilthead sea bream *Sparus aurata* L and sea bass *Dicentrarchus labrax* L. in Mediterranean coastal areas like Greece, Spain and Israel, and grouper, large yellow croaker, kuruma prawn, abalone and carpet shell clam throughout the world (Balebon *et al*., 1998a; Balebona *et al*., 1990; Aguirre-Guzman *et al*., 2004; Gu *et al*., 2016). Thus, *V. alginolyticus* represents a severe pathogen that raises public concerns and causes huge economic loss in aquaculture.

Antibiotics or other chemical agents have been applied in aquaculture farming like feeding additives and immersion baths to treat and prevent the spread of diseases including *V. alginolyticus* infection (Oh *et al*., 2011; Kang *et al*., 2016). However, the overuse or misuse of antibiotics leads to the selection of antibiotic-resistant bacteria (Manjusha *et al*., 2005). The antibiotic-resistant *V. alginolyticus* has been isolated from a variety of seafood, including fish and shellfish in the USA, China, Korea and many other countries (Cook *et al*., 2002; Lee *et al*., 2008; Zhao *et al*., 2011). Other methods like vaccination with live bacteria or inactivated bacteria represent an alternative approach, which gives high protection efficiencies. However, the development of effective vaccines is time and labour consuming. More importantly, the immunogens of microorganisms are always subject to mutations, making vaccine less effective (Ispasanie *et al*., 2018; Li *et al*., 2018). Thus, it is necessary to develop novel antibiotic-free approach for managing *V. alginolyticus* infection.

Although molecular steps involving in *V. alginolyticus* pathogenesis to seek for efficient control approaches have been extensively investigated, including the use of the model organism, *Danio rerio* (Zhao *et al*., 2014; Cheng *et al*., 2018a), metabolic mechanisms by which fish mount response to the infection is largely unknown. Recent reports have indicated that metabolic modulation is closely related to the host survival from bacterial infections (Ma *et al*., 2015; Chen *et al*., 2017; Zeng *et al*., 2017). Thus, effective approach based on metabolic modulation to eliminate bacterial pathogens without the use of antibiotics is promising. We have proposed a strategy that combines the use of functional metabolomics and metabolome re-programming to revert antibiotic-resistant bacteria to antibiotic-sensitive bacteria. When compared with kanamycin-sensitive *Edwardsiella tarda*, kanamycin-resistant *E. tarda* has reduced level of alanine, glucose, fructose and glutamate, which were subsequently used for metabolome re-programming. Exogenous alanine, glucose, fructose and glutamate re-sensitized the kanamycin-resistant *E. tarda* to kanamycin (Su *et al*., 2015; Peng *et al*., 2015a; Su *et al*., 2018). This strategy was further applied in other cases. Our laboratory and others demonstrated that phenylalanine, unsaturated linoleic acid, glucose, N-acetylglucosamine, L-Leucine, L-Proline and myo-inositol potentiate host's ability to clear pathogens like *V. alginolyticus, Streptococcus agalactiae*, balofloxacin-resistant *Escherichia coli* and *Streptococcus iniae* (Guo *et al*., 2014; Cheng *et al*., 2014; Chen *et al*., 2015; Zhao *et al*., 2015; Peng *et al*., 2015b; Jiang *et al*., 2018). In the present study, we aimed to seek potential metabolites that reduce the infection by *V. alginolyticus* in zebrafish. And the identified metabolite re-programs the host's metabolome to promote the host's survival. The metabolic mechanism of the re-programming is investigated and the consequent downstream effects are explored.

Results

The dying zebrafish from V. alginolyticus *infection display excessive immune response*

To develop an approach in managing bacterial infection, we adopted the *V. alginolyticus*-zebrafish interaction model by infecting *Danio rerio* with *V. alginolyticus*, at LD_{50} (Fig. S1). *D. rerio* began to die from 24 h post-infection and showed typical symptoms of bacteremia in fish, exemplifying as exophthalmos, ascites in abdominal cavity, skin discoloration, haemorrhagic in the wound and swelling spleen (Fig. 1A) as well as the increased number of bacteria in zebrafish homogenate (Fig. 1B). Most of the zebrafish died between 24 h and 48 h post-infection. No *D. rerio* died 60 h post-infection, where the mortality was monitored for a total of 14 days as previously adopted (Yang *et al*., 2018a; Fig. 1C). To investigate whether immune response contributed to the fish dying or survival, we measured the featured systematic increased immune mediators (Wen *et al*., 2018) including interleukin-1ß (*il-1b*), interleukin-6 (*il-6*), interleukin-8 (*il-8*), interleukin-10 (*il-10*) and TNF-α (*tnfa*) at 24 h post-infection due to the massive fish death after this time point. Both of the dying group and the survival group showed higher expression level of inflammatory cytokines than the saline group (Fig. 1D), but the expression of *il1b, il6, il8* and *tnfa* was higher in dying group than that in survival group (Fig. 1D), suggesting excessive immune response in the dying fish.

Immune response is associated with metabolic changes

Immune response is tightly linked to metabolism (Chen *et al*., 2017; Jiang *et al*., 2018). To develop an approach to elevate fish survival upon *V. alginolyticus* infection, we directly profiled the metabolomes of the dying group and the survival group through GC-MS based metabolomics. Ten individual zebrafish were collected for each group, and two technical replicates of each individual were examined. A total of 216 aligned peaks were identified in every sample from the control, dying and survival groups. After removing the internal standard, ribitol and other known solvents, 77 metabolites were identified. The correlation coefficients of the two technical repeats were between 0.995 and 0.999, indicating the reproducibility of the data (Fig. 2A). All of the identified metabolites were clustered together and displayed as heat map shown in Fig. 2B, and their folds of changes were summarized in Table S1. Among the identified metabolites, 30 metabolites were carbohydrates (39%), 24 metabolites were amino acid (31%), 11 metabolites were lipid (15%), 7 metabolites were nucleotide (9%) and 5 metabolites were unknown (6%; Fig. 2C).

To further explore the metabolic difference between the dying and survival groups, we adopted the Kruskal–Wallis test to compare the two groups to the saline group, whereas 61 metabolites and 62 metabolites of differential abundance were identified from the dying group and survival group, respectively. Unsupervised hierarchical clustering was applied to show the relative expression levels of those differential metabolites of the dying and survival groups to the saline group. We identified 37 increased metabolites and 24 decreased metabolites in the dying group, corresponding to Z value ranging from −4.43 to 24.14, where Z value represented the level of difference. Similarly, 37 increased metabolites and 25 decreased metabolites were identified in the survival group, corresponding to the Z value ranging from −3.89 to 13.49 (Fig. 2D). These data suggest that the dying group and survival group have differential metabolomes possibly related to different immune responses.

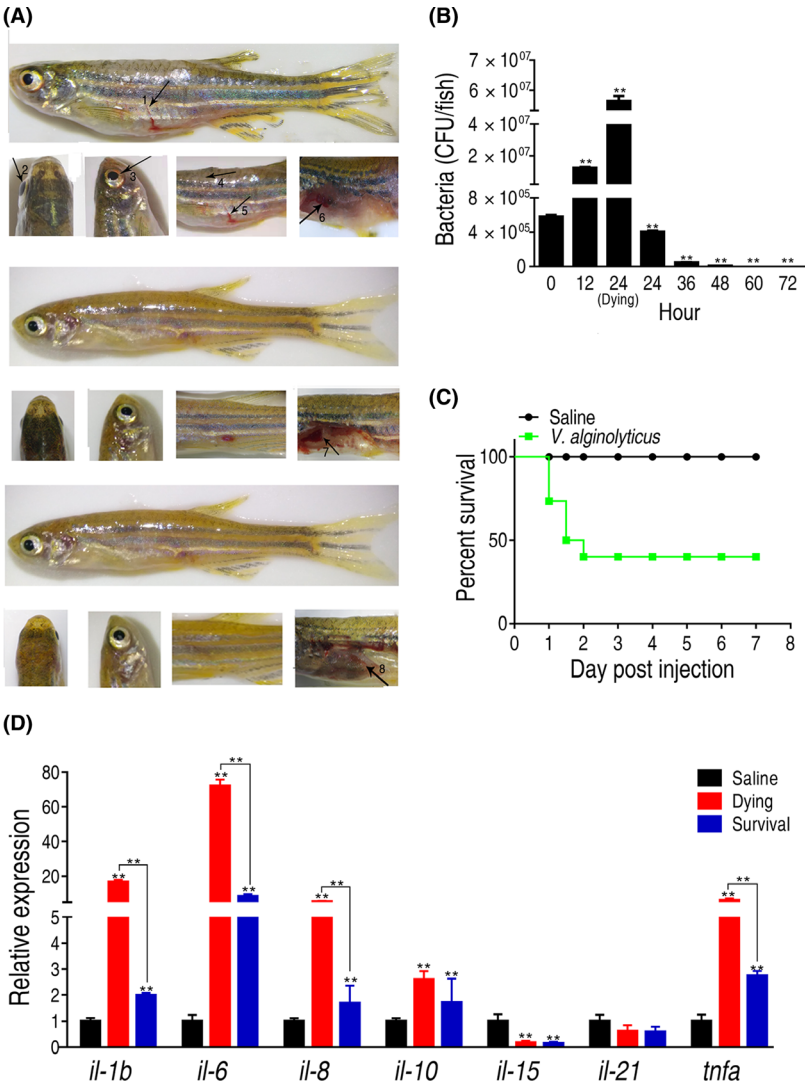

Fig. 1. *V. alginolyticus* infection was associated with excessive immune response in the dying fish.
A. Symptoms of dying (upper panel), survival (middle panel) and control (lower panel) *D. rerio* infected with *V. alginolyticus*. Arrow 1 showing ascites in the abdominal cavity; Arrows 2 and 3 showing exophthalmos in dying fish; Arrow 4 showing the disassociation of scales; Arrow 5 showing haemorrhagic in the wound; Arrow 6 showing the enlarged spleen in dying fish but not in survival fish (arrow 7) and control (arrow 8).
B. The amounts of bacteria in each fish at different time post-infection. Ninety zebrafish were randomly divided into three tanks with 30 zebrafish in each tank. After infection with bacteria at LD_{50}, two zebrafish were removed from each tank at the indicated time points. The fish were homogenized and the supernatant was collected for plating.
C. Percentage of survival of *D. rerio* infected with *V. alginolyticus* by Log-rank (Mantel–Cox) test. Zebrafish (n = 180) were randomly divided into two groups (n = 90 for each group; n = 30 in each tank representing one replicate). The fish was injected with either 5 μl saline (0.85% sodium chloride) or 5 μl *V. alginolyticus* (1.2×10^8 CFU ml^{-1}) per fish through intramuscular injection. Mortality was monitored for 14 days (only 7 days were shown as no death was observed after 7 days).
D. qRT-PCR for cytokine genes of control, dying or survival *D. rerio*. The spleens of control, dying or survival group were collected 24 h post-infection. For each group, three spleens were pooled for RNA isolation as one replicate. There were three replicates for each group (n = 9 for each group). All of the above statistic analyses were performed with Student's t test unless otherwise indicated. $^{*}P < 0.05$; $^{**}P < 0.01$. Error bars represent means ± SEM from at least three biological replicates.

Enrichment of metabolic pathways responsible for the dying or survival D. rerio

To investigate the metabolic pathways involved in *V. alginolyticus* infection, network analysis was performed for enrichment analysis with MetaboAnalyst. Fourteen pathways that had significant difference ($P < 0.05$) were enriched based on the differential metabolites, including phenylalanine, tyrosine and tryptophan biosynthesis, valine, leucine and isoleucine biosynthesis, glycine, serine and threonine metabolism, alanine, aspartate and glutamate metabolism, beta-Alanine metabolism, arginine and

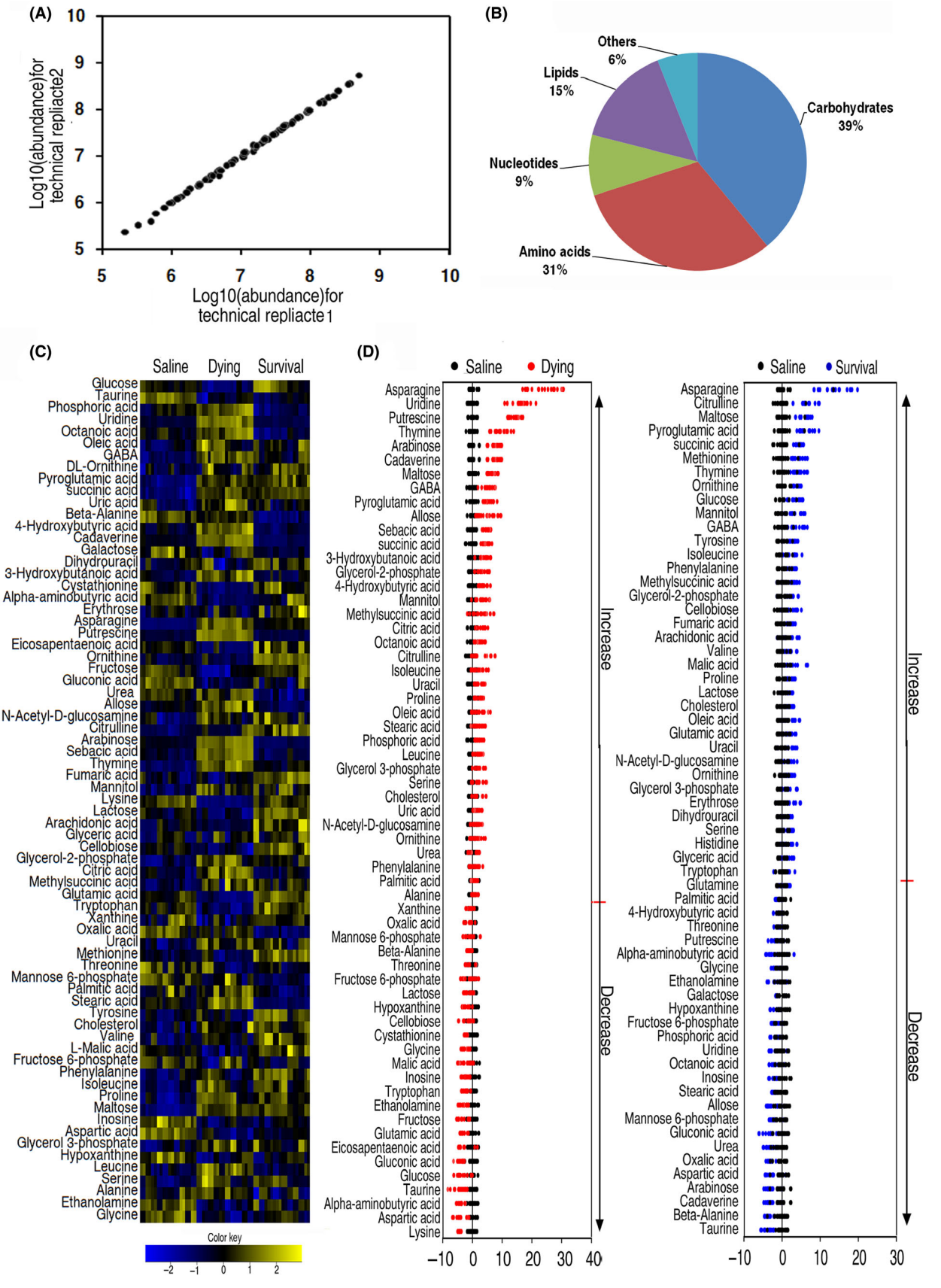

Fig. 2. Metabolomic analysis of control, dying and survival *D. rerio* upon *V. alginolyticus* infection. Twenty-four hours post-infection, fish from saline group ($n = 10$), dying group ($n = 10$) and survival group ($n = 10$) were collected to collect humoral fluids for GC-MS analysis.
A. Reproducibility of the data.
B. Heat map showing relative abundance of metabolites (Wilcoxon $P < 0.01$) in control, dying and survival groups. Heat map scale (blue to yellow: low to high abundance) is shown at bottom.
C. Functional categories of the identified metabolites.
D. *Z* scores (standard deviation from average) corresponding to data in (B).

proline metabolism, amino sugar and nucleotide sugar metabolism, citrate cycle (TCA cycle), aminoacyl-tRNA biosynthesis, glutathione metabolism, pantothenate and CoA biosynthesis, butanoate metabolism, nitrogen metabolism, cyanoamino acid metabolism, sorted by their weights (impact). The first phenylalanine, tyrosine and tryptophan biosynthesis pathway was the most impacted pathway (Fig. 3A). Among these enriched pathways, only two, phenylalanine, tyrosine and tryptophan biosynthesis, and butanoate metabolism, show that all metabolites detected are elevated (Fig. 3B). These results suggest that the elevated phenylalanine, tyrosine and tryptophan biosynthesis plays a role in fish survival.

Identification of crucial metabolites using multivariate data analysis

To identify the crucial metabolites in protecting *D. rerio* from killing by *V. alginolyticus*, orthogonal partial least square discriminant analysis (OPLS-DA) was applied. The three groups were clearly separated from each other. Component (t[1]) distinguished the infected groups from the saline group, whereas component (t[2]) distinguished the survival group from the dying group and the saline group (Fig. 3C). The cut-off values were set in OPLS-DA loadings plot for metabolites as greater or equal to 0.05 and 0.5 for absolute value of covariance p and correlation p(corr). As shown in Fig. 3D, each triangle represents a single differential metabolite, and the red triangles within the range of cut-off values were potential crucial biomarkers. The metabolites that differentiate the dying group from the survival group include phosphoric acid, stearic acid, uridine, palmitic acid, leucine, mannose-6-phosphate, valine, tryptophan, glutamic acid, tyrosine, phenylalanine and glucose. The ranking of these metabolites was provided in Table S2. To convert the crucial biomarkers into a predicting model of fish survival to *V. alginolyticus* infection, we analysed these metabolites with ROC curve, which were provided in Fig. S2. Tryptophan, glucose, glutamic acid and tyrosine showed the most significant value with a value > 0.9 for AUC, indicating these four metabolites could be predictive for the fish survival, which were provided in Table S2.

Among the differential metabolites, only tryptophan, glutamic acid and glucose are the ones that are downregulated in the dying group while are upregulated in survival group. Among the three increased metabolites, only tryptophan belongs to the most impacted pathway phenylalanine, tyrosine and tryptophan biosynthesis pathway. Therefore, tryptophan is identified as the most key metabolite for further functional study (Fig. 3E).

Central carbon metabolism is the key to fish survival or dying

We performed iPath analysis to compare metabolic pathways between the survival group and the dying group. The resulting global overview maps provide a better insight into the effects of the *V. alginolyticus* infection on the whole metabolism of zebrafish, where red line represents increased metabolic pathways and green line represents the decreased metabolic pathways. We identified the elevation of the most metabolic pathways network, including the TCA cycle and energy metabolism in the survival group, implying the importance of the activation of the TCA cycle and promotion of the energy metabolism for zebrafish survival (Fig. 4B). In the contrast, completely different metabolic pathways were determined in the dying group (Fig. 4A). To confirm such metabolic flow, we measured the activity of pyruvate dehydrogenase (PDH), succinate dehydrogenase (SDH), α-Ketoglutarate dehydrogenase (α-KGDH) and malate dehydrogenase (MDH) in the dying and survival groups. Consistently, all enzymatic activities were lower in dying group than the saline group and survival group. More importantly, the enzymatic activities in survival group were higher than those in saline group (Fig. 4C). These results indicate that inactivation and activation of the TCA cycle in the dying and the survival groups, respectively, which is related to tryptophan levels in the two groups.

Tryptophan promotes the TCA cycle to increase D. rerio *survival against* V. alginolyticus *infection*

To examine the potential effect of tryptophan on *V. alginolyticus* infection, we treated *D. rerio* with tryptophan by intraperitoneal injection for 6 days, the control group was injected with saline, and then followed with bacterial challenge at LD_{50}. Tryptophan increased fish survival up to 23.7% (Fig. 5A). The metabolic mechanism that

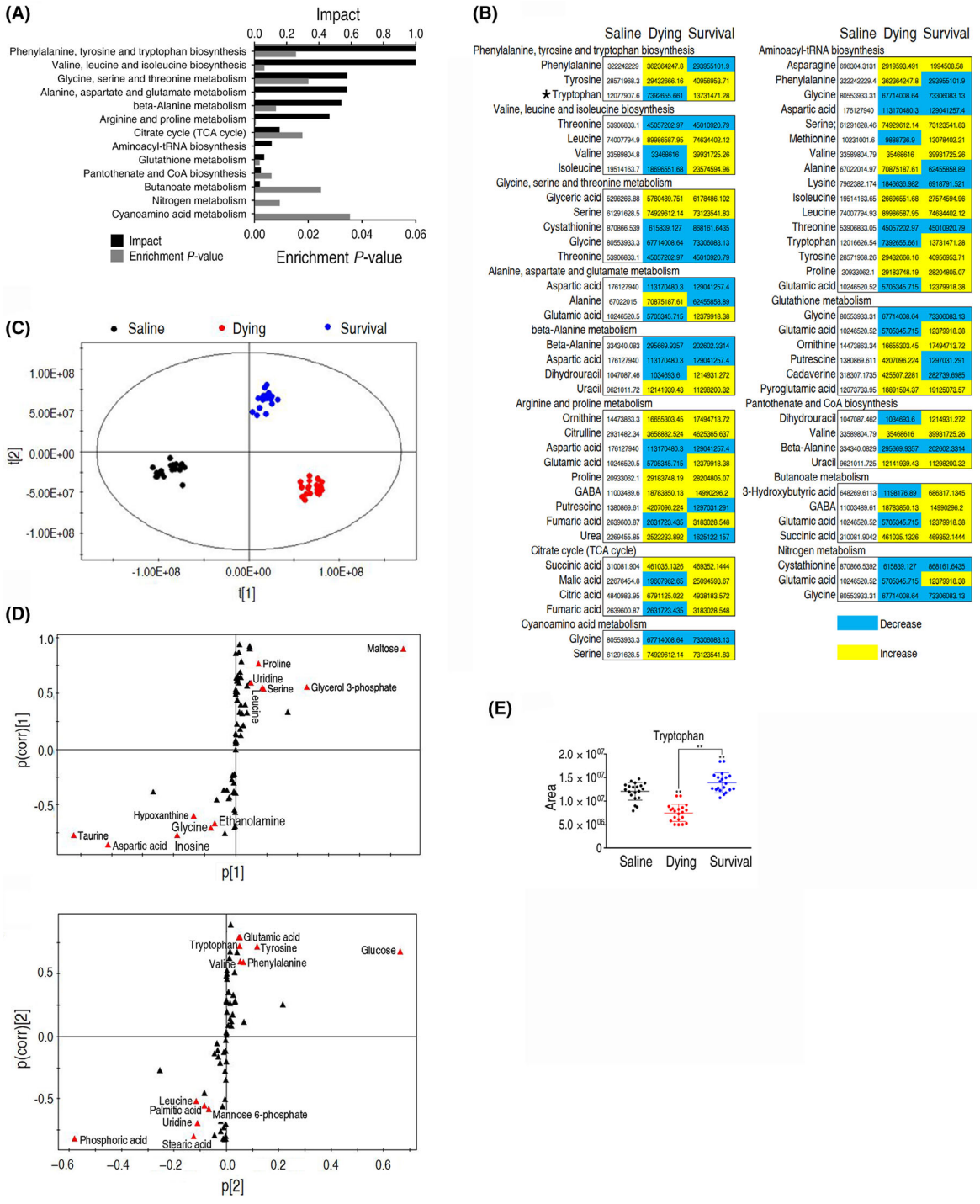

Fig. 3. Enriched pathways and crucial biomarkers between dying and survival groups.
A. Pathway enrichment analysis of differential metabolites. To investigate the metabolic pathways, the metabolites of differential abundance were selected and analysed in MetaboAnalyst to enrich pathways. Fourteen pathways that had significant difference ($P < 0.05$) were enriched and sorted by their weights (impact).
B. Change of the abundance of the metabolites. The lists of the 75 metabolites enriched in the fourteen pathways in (A). Yellow indicates increase; Blue indicates decrease.
C. Principle component analysis of control, dying and survival *D. rerio*. Each dot represented one technical replicate.
D. The distribution of differential abundance of metabolites' weight from method of OPLS-DA to control and experimental samples. Triangle represented metabolites and candidate biomarkers were highlighted with red.
E. Abundance of tryptophan in saline, dying and survival. Statistical analysis was performed with Student's *t* test, $^{*}P < 0.05$; $^{**}P < 0.01$. Error bars represented means ± SEM from at least three biological replicates.

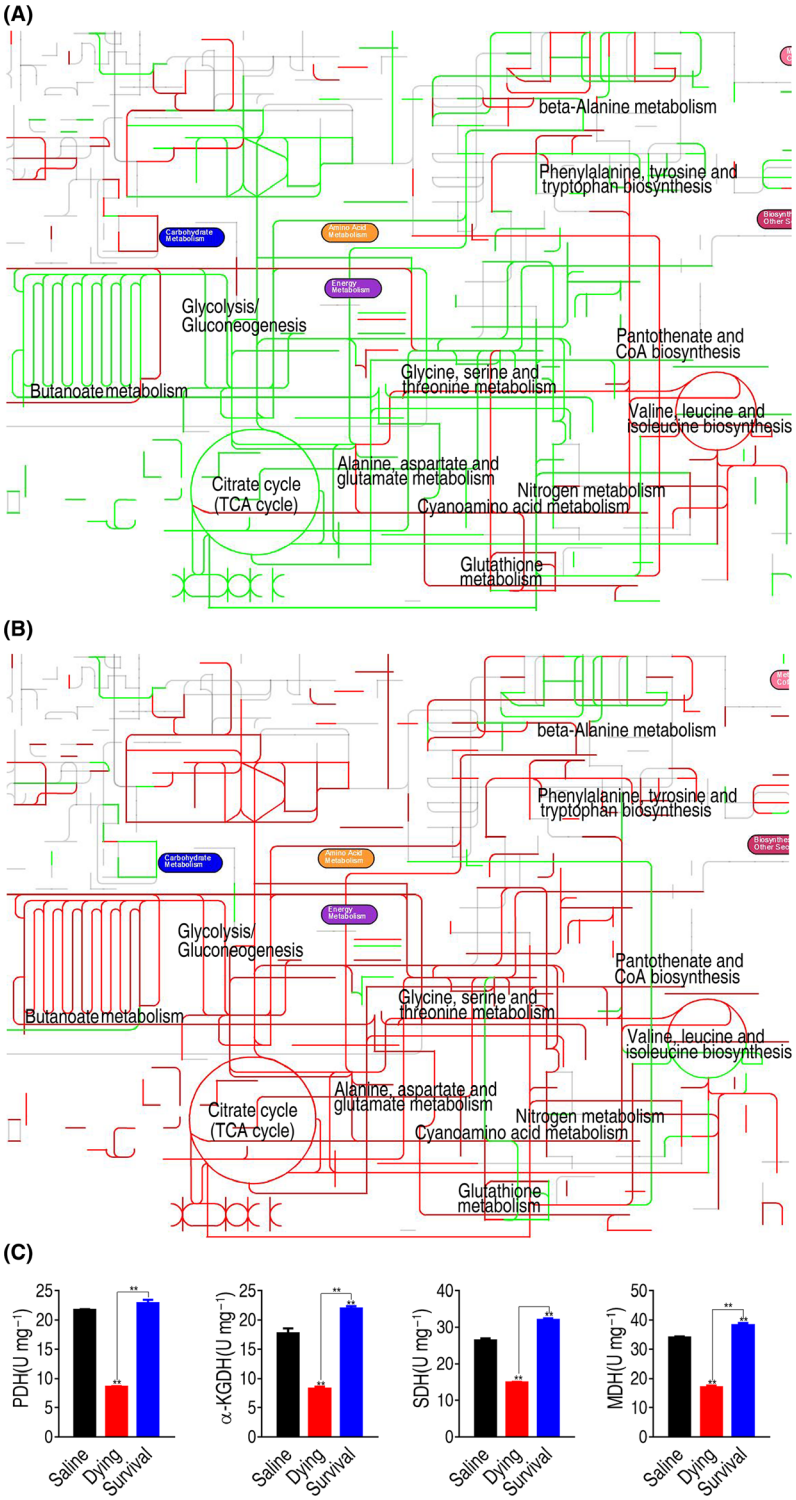

Fig. 4. iPath analysis and activity of enzymes in dying and survival groups.
A,B. iPath analysis of the metabolites of differential abundance in the dying group and survival group, respectively. Red and green lines represented increase and decrease of metabolism, respectively.
C. Enzymatic analysis of PDH, KGDH, SDH and MDK in saline, dying and survival *D. rerio*. The visceral organ homogenates of saline, dying or survival group were collected 24 h post-treatment. For each group, the homogenates from three zebrafish were pooled for enzyme analysis. There were three replicates for each group ($n = 9$ for each group). Statistical analysis was performed with Student's *t* test, $^{**}P < 0.01$. Error bars represent means ± SEM from at least three biological replicates.

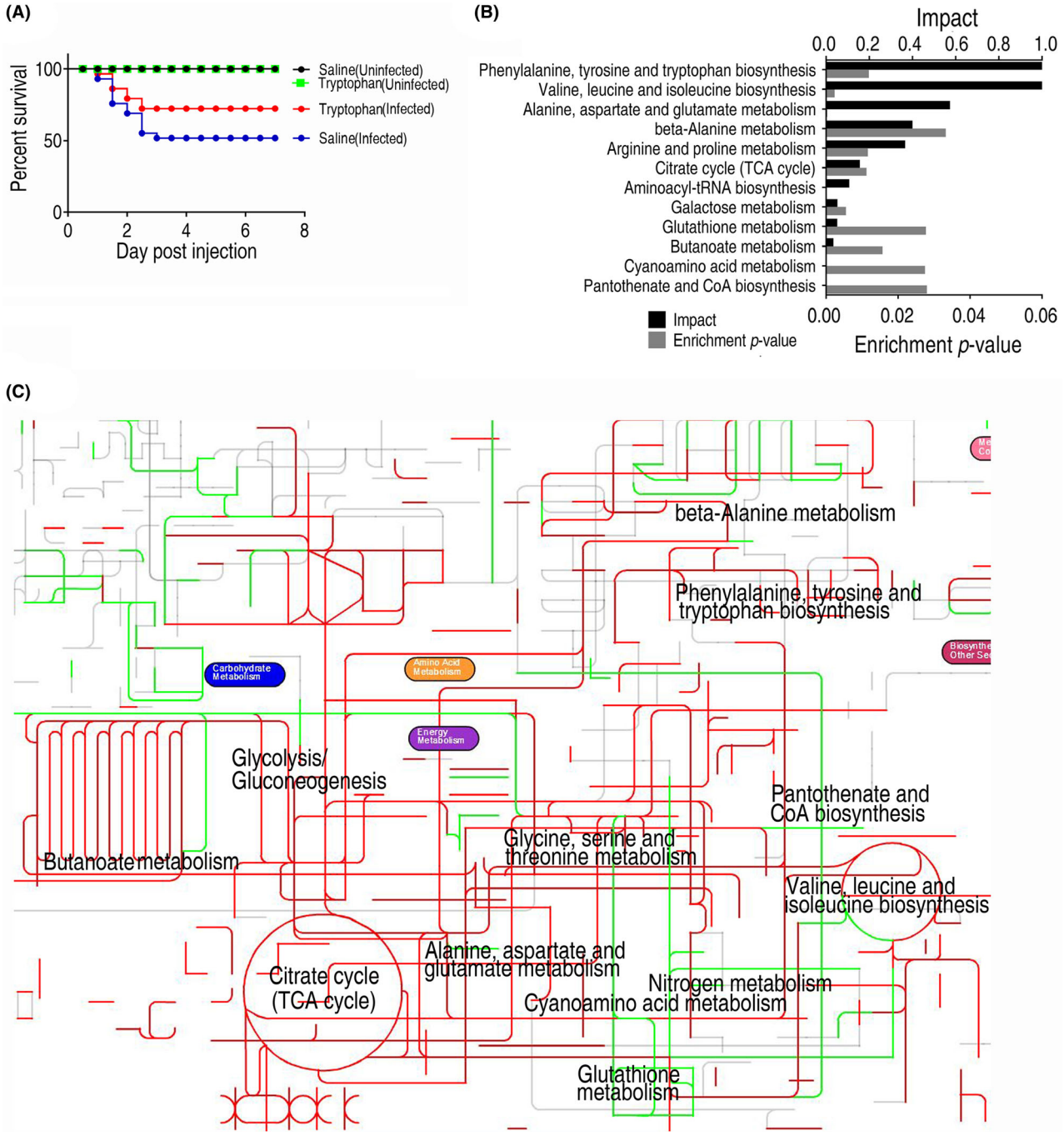

Fig. 5. Tryptophan protects *D. rerio* against *V. alginolyticus* infection.
A. Percentage of survival of *D. rerio* pretreated with tryptophan by Log-rank (Mantel–Cox) test. A total of 240 zebrafish were used. Zebrafish were injected with saline only (n = 30) or 5 μl 50 mM tryptophan only (n = 30) or saline (n = 90; n = 30 per tank as one replicate) once a day for 6 days followed by *V. alginolyticus* with 5 μl (1.2×10^8 CFU ml) per fish or tryptophan (n = 90; n = 30 per tank as one replicate) once a day for 6 days followed by *V. alginolyticus* infection at the same dose through intramuscular injection. Saline or tryptophan was given through intraperitoneal injection. The mortality was monitored for 14 days post-infection (only 7 days were shown as no death was observed after 7 days).
B. Metabolic pathway enrichment analysis of *D. rerio* treated with tryptophan. Twenty-four hour after tryptophan injection, fish from saline control (n = 10) and tryptophan group (n = 10) were collected to collect humoral fluids for GC-MS analysis.
C. iPath analysis in tryptophan-treated group. The metabolite of differential abundance to control group were applied in iPath. Red and green lines represented increase and decrease of metabolism, respectively.

tryptophan enhanced host survival was investigated through metabolomics. Each individual of *D. reiro* was treated with 5 μl 50 mM tryptophan or 5 μl saline as experimental group and control group, respectively. Both of the two groups were injected once daily for 6 days, and *D. reiro* were collected for GC-MS analysis after the last treatment. Ten *D. rerio* were collected from each group and a total of 75 metabolites were identified, where 69 differential metabolites were identified by Mann–Whitney U tests (Fig. S3), and their folds of change were summarized in Table S3. The differential metabolites were analysed by pathway analysis that enriched ten metabolic pathways (Fig. 5B).

Furthermore, the comparative metabolic pathway analysis between the zebrafish with and without tryptophan was carried out in iPath, where red line represents increased metabolic pathways and green line represents the decreased metabolic pathways. The tryptophan-mediated global overview map provides a better insight into the whole metabolism impacted by exogenous tryptophan. Comparatively, the tryptophan-mediated map is similar to the survival global overview map described above (Figs. 4B and 5C). These results indicate that exogenous tryptophan promotes host to mount an anti-infective metabolome.

One of the enriched pathways was the TCA cycle. Tryptophan activates mTOR to promote glycolysis and TCA cycle via pyruvate and acetyl-CoA (Düvel *et al.*, 2010; Dukes *et al.*, 2015; Gong *et al.*, 2018). To confirm such metabolic flow, we detected the activity of hexokinase (HK), 6-phosphofructokinase (PFK), pyruvate kinase (PK) in the glycolysis, of pyruvate dehydrogenase (PDH) in the pyruvate metabolism and of α-KGDH, succinate dehydrogenase (SDH) and MDH in the TCA cycle in zebrafish with and without tryptophan. Indeed, the treatment of fish with tryptophan increased the activity of HK, PFK, PK, PDH, α-KGDH, SDH and MDH (Fig. 6A and B). HK phosphorylates hexoses, forming hexose

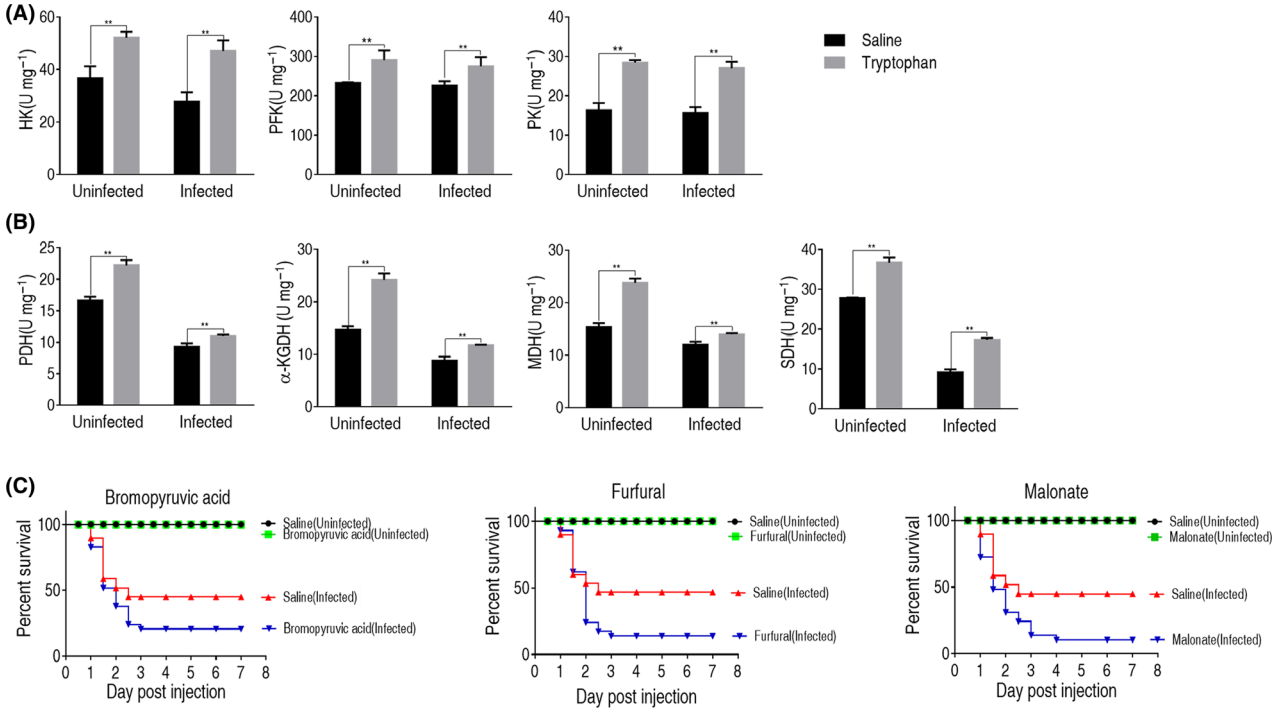

Fig. 6. Tryptophan-induced glycolysis, pyruvate metabolism and the TCA cycle and the effect on bacterial survival.
A. Enzymatic analysis of HK, PEK and PK in the presence of tryptophan and bacterial infection.
B. Enzymatic analysis of PDH, KGDH, SDH and MDK in the presence of tryptophan and bacterial infection.
C. Percentage of survival of *D. rerio* when TCA cycle was blocked by inhibitors. Zebrafish (n = 360) were randomly divided into four groups (n = 90 for each group; n = 30 in each tank representing one replicate). The fish were injected with 5 μl saline or bromopyruvate (2.5 mM), furfural (50 mM) or malonate (12.5 mM) through intraperitoneal injection, followed by bacterial challenge with 5 μl *V. alginolyticus* (1.2×10^8 CFU ml^{-1}) per fish through intramuscular injection. Zebrafish (n = 120) were injected with saline only (n = 30) or furfural only (n = 30) or bromopyruvic only (n = 30) or malonate only (n = 30) through intraperitoneal injection. Mortality was monitored for 14 days and analysed by Log-rank (Mantel–Cox) test (only 7 days were shown as no death was observed after 7 days). All of the above statistic analysis unless otherwise stated was performed with Student's t test unless otherwise indicated. $^{*}P < 0.05$; $^{**}P < 0.01$. Error bars represent means ± SEM from at least three biological replicates.

phosphate. PFK phosphorylates fructose 6-phosphate. PK catalyses the transfer of a phosphate group from phosphoenolpyruvate to adenosine diphosphate, yielding one molecule of pyruvate and one molecule of ATP the final step of glycolysis. PDH is the key enzyme in the formation of pyruvate and acetyl-CoA. We treated *D. rerio* with two different PDH inhibitors, furfural and bromopyruvate, and with one inhibitor malonate to succinate dehydrogenase (SDH), which is an enzyme in TCA cycle. The inhibition of PDH with bromopyruvate and furfural and the inhibition of SDH with malonate decreased the survival rates by 23.3% in bromopyruvate, 30% in furfural and 33.3% in malonate (Fig. 6C). These results imply that pyruvate dehydrogenase and the TCA cycle play positive roles in fencing against *V. alginolyticus* infection.

Tryptophan decreased ROS production by modulating NADPH generation and oxidation

The TCA cycle mainly occurs in mitochondria and generates ATP for cellular activity. ATP serves as a substrate for NADH kinase to generate NADPH, whose oxidation is the primary sources for ROS production. Meanwhile, the burst expression of pro-inflammatory cytokines increases of ROS production which may also damage host tissues.

To investigate whether tryptophan may engage in the control of cytokine-induced ROS, we quantify the ROS production after the bacterial infection. Interestingly, ROS was significantly increased with bacterial infection, while the ROS in the dying group was much higher than that in survival group (Fig. 7A). However, the treatment of fish with tryptophan significantly decreased the ROS ($P < 0.01$) when challenged with bacteria but the less effect without bacterial challenge ($P < 0.05$; Fig. 7B). These data suggest that tryptophan protects zebrafish against pathogen through its antioxidant activity.

The ATP level was lower in dying group than the saline and survival group but was higher in survival group than saline group ($P < 0.01$; Fig. 8A). Tryptophan increased the ATP concentration significantly with bacteria challenge ($P < 0.01$; Fig. 8B). In addition, the expression of *nox-1*, the NADPH oxidation enzymes, was increased two folds in the dying group than the saline group ($P < 0.01$; Fig. 8C). Interestingly, exogenous tryptophan did not change the expression of *nox-1* when challenged with bacteria, indicating tryptophan might trim *nox-1* expression to an appropriate level ($P < 0.01$; Fig. 8D). Meanwhile, the level of NADPH is lower in the dying group than that in saline or survival group ($P < 0.01$; Fig. 8E) but was increased in the presence of tryptophan ($P < 0.01$; Fig. 8F). Low NADPH represents low antioxidant level. These data together suggest that tryptophan modulates ROS production in protecting host death during immune response to *V. alginolyticus* infection.

Discussion

The control of bacterial infection becomes an emergent topic worldwide due to the widespread of antibiotic-resistant bacteria in the world. Antibiotic resistance thus represents catastrophic threat to humans, especially for immunocompromised patients in clinics. One of the major sources of antibiotic contaminants is from fish farming and poultry industry (Dubreil *et al.*, 2017). The use of antibiotics to prevent and treat bacterial infection is the routine way. Although the discovery of new classes of antibiotics that might be used to overcome the current antibiotic resistance, the pipeline for such development is still too long to combat with the current rapid generation of antibiotic-resistant strains. Thus, the development of new strategy to deal with bacterial infection independent of antibiotics is urgent.

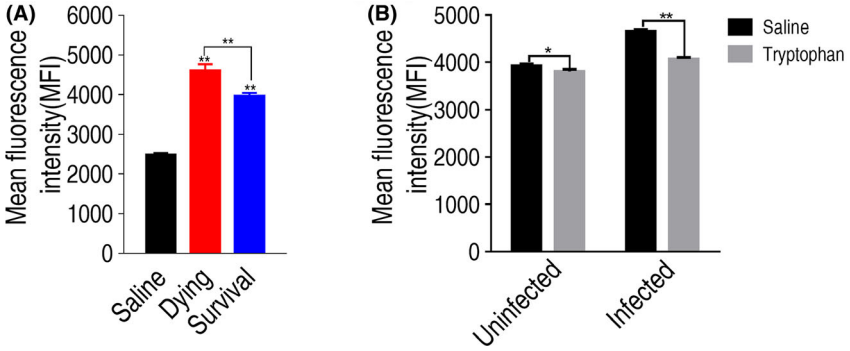

Fig. 7. Tryptophan attenuates ROS production in *D. rerio*.
A. ROS production in saline, dying and survival *D. rerio.*
B. ROS production in the presence of tryptophan upon bacterial infection. For the above experiments, the visceral organ homogenates of saline, dying or survival group were collected 24 h post-treatment. For each group, the homogenates from three zebrafish were pooled for ROS quantification. There were three replicates for each group ($n = 9$ for each group). All of the above statistic analysis was performed with Student's *t* test unless otherwise indicated. $^{*}P < 0.05$; $^{**}P < 0.01$. Error bars represented means ± SEM from at least three biological replicates.

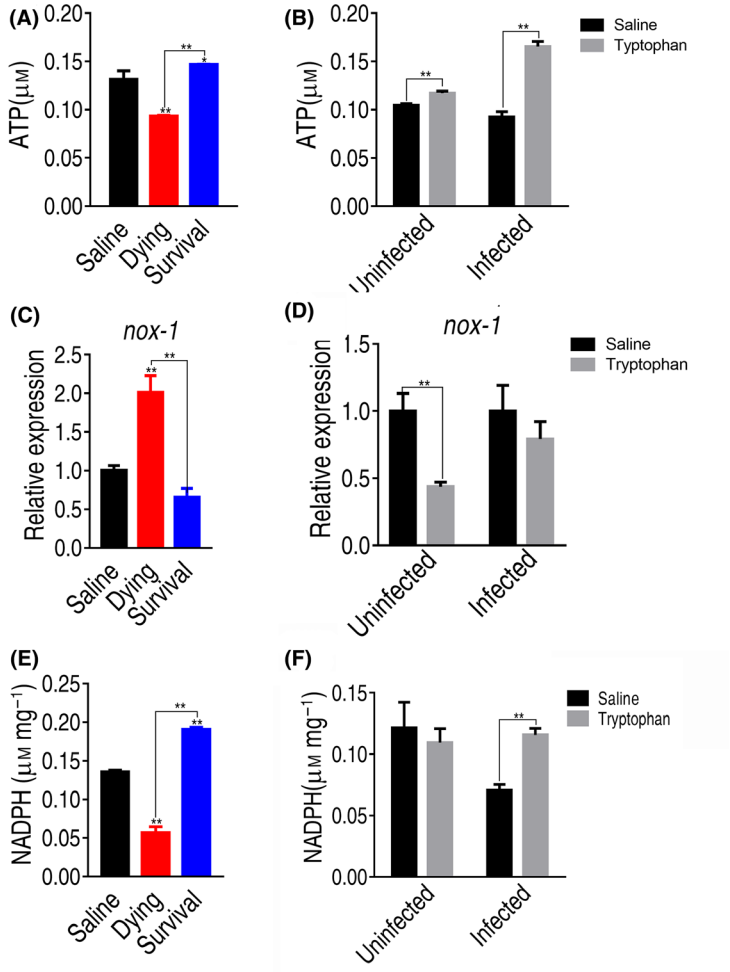

Fig. 8. Tryptophan attenuates ROS production through TCA cycle. (A, B) Quantification of ATP in control, dying and survival *D. reiro* (A) or in the presence of tryptophan (B) upon bacterial infection. (C) qRT-PCR of *nox-1* transcription in saline, dying and survival *D. reiro* or (D) in the presence of tryptophan upon bacterial infection. (E) Quantification of NADPH in saline, dying and survival *D. reiro* or (F) in the presence of tryptophan upon bacterial infection. For the above experiments, the spleens of saline, dying or survival group were collected 24 h post-treatment. For each group, three spleens were pooled for qRT-PCR analysis, the visceral organ homogenates of saline, dying or survival group were collected 24 h post-treatment. For each group, the homogenates from three zebrafish were pooled for ATP quantification and NADPH. There were three replicates for each group ($n = 9$ for each group). All of the above statistic analysis was performed with Student's *t* test unless otherwise indicated. $^{*}P < 0.05$; $^{**}P < 0.01$. Error bars represented means ± SEM from at least three biological replicates.

Vibrio bacteremia is one of the major causes of fish death after Vibrio infection, which is always accompanied with septic shock, featured with overactive immune response (Fu *et al.*, 2016). In the present study, we found that *V. alginolyticus* infection caused fish death associated with an excessive interleukin secretion. Cytokine can trigger tissue damage due to the production of massive ROS in the host (Yang *et al.*, 2007). Immune activation is tightly regulated by metabolism (Ganeshan and Chawla, 2014). The present study compared the metabolic profiles of *D. rerio* that were died of and that were survived from infection. Interestingly, we found that these two groups had distinct metabolome profiles, which implied that metabolic state determines the fate of the host that is succumbed to the infection or not. By multivariate analysis, we identified tryptophan as the crucial biomarker that was higher in the survival and lower in the dying, indicating that the level of the biomarker is closely related to the consequence of zebrafish infected by *V. alginolyticus* infection. Tryptophan is an essential amino acid that is required by all forms of life for protein synthesis and other macromolecule synthesis (Moffett and Namboodiri, 2003). The breakdown of tryptophan generates kynurenines through tryptophan catabolism has immunomodulatory functions (Cervenka *et al.*, 2017), known as kynurenines pathway (KYN). Several reports have indicated KYN in infections of virus, parasite and bacteria. Alteration of KYN pathways have been observed in HIV-, hepatitis B- virus and hepatitis C-infected infected patients (Chen and Guillemin, 2009)

and also in toxoplasma-infected patients (Groer *et al*., 2011). More importantly, the KYN pathway is markedly induced during bacterial infections such as tuberculosis or bacterial sepsis (Huttunen *et al*., 2010). However, information regarding the action of tryptophan against Vibrio infection and the anti-infection in fish is unknown. Tryptophan is nutritious to human and fish and can be conveniently used, especially used as feeding additives in aquaculture. Thus, modulating microenvironment by metabolites could be one of the major ways in regulating host response to infections.

Our recent reports have indicated that the metabolites-enabled killing of bacterial pathogens by antibiotic or hosts is attributed to metabolome re-programming (Peng *et al*., 2015c; Yang *et al*., 2018a; Yang *et al*., 2018b). The metabolome re-programming makes the antibiotic-resistant metabolomes to the antibiotic-sensitive metabolomes, thereby promoting antibiotic uptake and elevating antibiotic efficacy (Peng *et al*., 2015b). Meanwhile, we have also showed that these metabolites can re-programme the metabolomes to restore host' ability against bacterial pathogens (Yang *et al*., 2018a), but the mechanisms are largely unknown. The present study detected the metabolome re-programmed by tryptophan to understand the metabolic mechanisms. Reports indicate that tryptophan activates mTOR, which in turn promotes the glycolysis and TCA cycle (Düvel *et al*., 2010; Dukes *et al*., 2015; Gong *et al*., 2018). To demonstrate this, we detected the increased the activity of HK, PFK and PK in glycolysis, of PDH in pyruvate metabolism and of SDH, α-KGDH and MDH in the TCA cycle. This is further supported by the following findings that the higher and lower tryptophan was related to the activated and inactivated TCA cycle in the survival and dying fish, respectively, in the present study. The promoted TCA cycle in fighting against Vibrio infection is consistent with a previous result (Yang *et al*., 2018a). These results indicate that the activation of the TCA cycle is required for zebrafish against infection caused by *V. alginolytocus*.

Moreover, the present study explores the downstream mechanisms regulated by the re-programmed TCA cycle. The TCA cycle is in turn promoting the production of ATP. ATP level was lower in the dying than the survival, whereas tryptophan promoted ATP level, which was increased due to *V. alginolyticus* challenge. ATP is the substrate for producing NADPH, and the level of NADPH represents the antioxidant capability of the cell. Similarly, NADPH level was lower in the dying than the survival, while tryptophan increased NADPH level. These results support the conclusion that tryptophan activates the TCA cycle, promotes ATP production, elevates NADPH level (under *V. alginolyticus* infection), thereby ameliorating ROS to increase the survival. We, thus, report a new function of tryptophan in immune response that modulates the function of TCA cycle to increase NADPH level but decrease NADPH oxidation (Fig. 9).

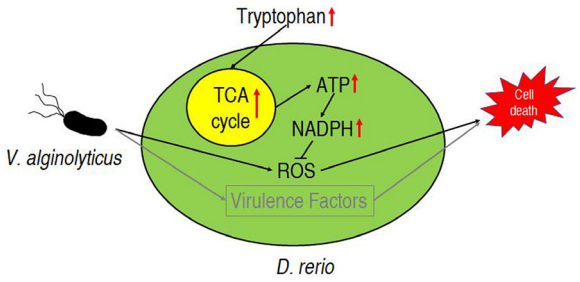

Fig. 9. The proposed model. The *V. alginolyticus* infection causes *D. reiro* death through virulence factors and septic shock-associated oxidative stress. The oxidative stress could be relieved by tryptophan, which fluxes into the TCA cycle to increase the ATP production. ATP served as the substrates for the production of NADPH, which antagonized the ROS, thus protecting host death from overactive immune response like ROS.

The concentration of exogenous tryptophan is 50 μg per zebrafish per day, which equals 0.25 mg g^{-1} day^{-1}. Although this concentration is higher than the physiological level, which fluctuates between 5 and 30 μM, we did not observe any abnormal manifestation at this concentration. Meanwhile, there are ample evidences that higher concentration that ~ 1100 mg tryptophan day^{-1} from dietary protein ingested in men (Fernstrom, 2016) or 300 mg kg^{-1} day^{-1} of tryptophan injected into rats are nontoxic (Moffett *et al*., 1998). Therefore, the concentration we used in this study is safety to zebrafish. Moreover, we expect the fish survival would increase in a tryptophan dose-dependent manner. The reason is that we have previously shown that the administration of exogenous threonine, taurine and palmitic acid increased fish survival against *Edwardsiella tarda* infection at higher temperature in a time-dependent manner (Jiang *et al*., 2019). However, we should be aware that this protective potency of tryptophan would achieve thresh hold at certain concentration due to the negative feedback of metabolic pathways (Sas *et al*., 2018).

In addition to tryptophan, there are other metabolites with increased abundance in survival fish including glucose, glutamic acid, tyrosine, phenylalanine and valine. These metabolites are potential to potentiate fish survival as glucose has been proved to be effective in boosting immunity to *E. tarda* infection (Zeng *et al*., 2017), phenylalanine can increases lysozyme production to eliminate antibiotic-resistant bacteria (Jiang *et al*., 2018), and valine increases macrophages phagocytosis to clear bacterial infection (Chen *et al*., 2017). Although the role of glutamic acid and tyrosine in immune response in fish has not been extensively investigated, we speculate that they could play protective role as they can enter the

TCA cycle to increase ATP production as did by tryptophan, which however waits for further investigation.

In conclusion, our study has reported the use of re-programming metabolomics to investigate how fish host mounts metabolic strategy to cope with *V. alginolyticus* infection. The hosts that survived or died of the infection are substantially different on their metabolomes, which could be adjusted by exogenous addition of the crucial metabolites, like tryptophan in our study. Although we only demonstrate the pretreatment of tryptophan before infection increased fish survival, we expect this effect also works injected at the beginning of infection, which waits for further investigation. Therefore, the use of metabolite is of great potential to enhance host's immunity to infections, thus representing a novel strategy to manage bacterial infections in an antibiotic-independent approach.

Experimental procedures

Bacterial strain and fish

Vibrio alginolyticus 12G01 (GenBank accession Nos. AAPS01000007) was isolated from Plum Island Ecosystem-LTER, USA, from surface waters by plating. *V. alginolyticus* 12G01 is a marine microbe associated with soft tissue infections, leading to bacteremia. *V. alginolyticus* 12G01 is grown in Luria–Bertani (LB) broth plus additional 4% of sodium chloride at 30°C.

Zebrafish (0.2 ± 0.03 g body weight), *Danio rerio*, were obtained from a zebrafish breeding Corporation (Guangzhou, China). These animals were free of *Vibrio species* infection through microbiological detection. A total of 1200 zebrafish were reared in 40 water tanks (25 l), where 30 individual zebrafish were reared in each tank equipped with Closed Recirculating Aquaculture Systems, and the maintaining physico-chemical parameters were as follows: water temperature: 27–29°C, dissolved oxygen: 6–7 mg l^{-1}, carbon dioxide content: < 10 mg l^{-1}, pH value: 7.0–7.5, nitrogen content: 1–2 mg l^{-1} and nitrite content: 0.1–0.3 mg l^{-1}. These animals were cultured under this condition for two weeks before experimental manipulation and were fed twice daily with commercial fish feed (38% crude protein, 6% crude fat and 16% crude ash related to wet matter, 7% crude fibre and 8% moisture, based on NRC recommendations, at a ratio of 3% of body weight per day) on a 12 h/12 h rhythm of light and darkness photoperiod always. The tank was cleaned twice a day by siphoning up the food debris and faeces.

Ethics statement

This study was conducted in accordance with the recommendations in the Guide for the Care and Use of Laboratory Animals of the National Institutes of Health and maintained according to the standard protocols (http://ZFIN.org). All experiments were approved by the Institutional Animal Care and Use Committee of Sun Yat-sen University (Animal welfare Assurance Number: 16).

Bacterial challenge and sample preparation for GC-MS analysis

Sample preparation was carried out as described previously (Zhao *et al*., 2014). Zebrafish (n = 180) were randomly divided into two groups, the control group (n = 90) and bacterial infection group (n = 90). For each group, the fish were further randomly divided into three subgroups (n = 30) representing three replicates, where each subgroup was reared in an individual tank. The control group was injected with 5 μl saline per fish (0.85% sodium chloride) while the bacterial infection group was injected with 5 μl *V. alginolyticus* (1.2×10^8 CFU ml^{-1}) per fish through intramuscular injection (by inserting the needle into the left tail muscle for 2–3 mm and no < 45° from the body in horizontal) as infection group. Ten saline-injected fish, ten dying fish and ten survived fish were collected 24 h post-injection for GC-MS analysis.

To prepare fish sample for GC-MS analysis, *D. rerio* was rinsed thoroughly with distilled water and then wiped thoroughly with sterilized gauze. These animals were cut into five pieces on ice and then weighted. The appropriate volume of saline (100 μl/100 mg) was added according to the weight, 4°C, overnight. After centrifugation at 3000 *g* for 10 min at 4°C, 100 μl supernatant was isolated for extraction of metabolites, where the supernatant from each fish was one biological sample and for each biological sample with two technical replicates.

GC-MS analysis

GC-MS analysis was carried out with a variation on the two-stage techniques as described previously (Yang *et al*., 2018a). In brief, samples were derivatized and then used to first protect carbonyl moieties through methoximation, through a 90 min, 37°C reaction with 80 μl of 20 mg ml methoxyamine hydrochloride (Sigma-Aldrich, St. Louis, MI, USA) in pyridine, followed by derivatization of acidic protons through a 30 min of 37°C reaction with the addition of 80 μl of N-methyl-N-trimethylsilyltrifluoroacetamide (MSTFA, Sigma-Aldrich). The derivatized sample of 1 μl was injected into a 30 m × 250 μm i.d. × 0.25 μm DBS-MS column using splitless injection, and analysis was carried out by Agilent 7890A GC equipped with an Agilent 5975C VL MSD detector (Agilent Technologies, Santa Clara, CA, USA). The initial temperature of the GC oven was held at 85°C for 5 min followed by an increase to 270°C at a rate of 15°C min^{-1} then held for 5 min. Helium was used as carrier gas and flow was kept constant at 1 ml min^{-1}. The MS was operated in a range of 50–600 m/z. For each sample, two technical replicates were prepared to confirm the reproducibility of the reported procedures.

Data processing and statistical analyses

GC-MS data were analysed as previously described (Yang *et al*., 2018a). Chromatography deconvolution and calibration were performed with AMDIS and internal standards. Raw data were filtered and then compiled to retention time correction and peak alignment. A file with the abundance

information of every metabolite in all samples was assembled thereafter, which was used to retrieve in National Institute of Standards and Technology (NIST 8.0) Mass Spectral Library and then subjected to metabolite identification. Each resolved peak area was normalized by internal standard ribitol and then a single matrix with RT-m/z pairs for each file was formed by the resulting peak intensity. This file was used for subsequently statistical analysis.

Metabolites data subtracted the medium metabolites and were scaled by the quartile range in the sample. Z-score analysis was used to scale each metabolite according to a reference distribution and calculated based on the mean and standard deviation of reference sets control. Hierarchical clustering was performed on quartile normalize date, completed in the R platform with the package gplots (http://cran.r-project.org/src/contrib/Descriptions/gplots.html) using the distance matrix. The normalized data were analysed by principal component analysis (PCA; SIMCA-P + 12.0.1), orthogonal partial least squares discriminant analysis, (OPLS-DA) could distinguish sample patterns, identify the metabolites associated with infection and to minimize the inter-individual variation's influence. SPSS 13.0 and Prism v5.01 (GraphPad, La Jolla, CA) were used to draw the histogram of the scatter plot. To further evaluate the reliability of the biomarker, a receiver operating characteristics (ROC) was built by SPSS 17.0.

Exogenous administration of tryptophan and bacterial challenge

A total of 240 zebrafish were used. Zebrafish were injected with saline only ($n = 30$) or 5 μl 50 mM tryptophan only ($n = 30$) or saline ($n = 90$; $n = 30$ per tank as one replicate) once a day for 6 days followed by *V. alginolyticus* with 5 μl (1.2×10^8 CFU ml^{-1}) per fish or tryptophan ($n = 90$; $n = 30$ per tank as one replicate) once a day for 6 days followed by *V. alginolyticus* infection at the same dose through intramuscular injection. Saline or tryptophan was given through intraperitoneal injection. The rationale for the injection method was followed as previously described (Karami *et al*., 2011). The mortality was monitored for 14 days post-infection.

For the effects of the TCA cycle on host survival, a total of 360 zebrafish were randomly divided into four groups. For each group, the fish were further randomly divided into three subgroups ($n = 30$) representing three replicates, where each subgroup was reared in an individual tank. The control group was injected with 5 μl saline per fish (0.85% sodium chloride) while the other three groups were treated with TCA cycle inhibitors bromopyruvate (2.5 mM), furfural (50 mM) or malonate (12.5 mM) once per day for three days through intraperitoneal injection, followed by bacterial challenge with 5 μl *V. alginolyticus* (1.2×10^8 CFU ml^{-1}) per fish through intramuscular injection (by inserting the needle into the left tail muscle for 2–3 mm and no less than 45° from the body in horizonal). In addition to the 360 zebrafish, another 120 zebrafish were injected with saline ($n = 30$) or one of the inhibitors only ($n = 30$ for each inhibitor group through intraperitoneal injection). Mortality was monitored for 14 days and analysed by Log-rank (Mantel–Cox) test.

Quantification of reactive oxygen species

The production of ROS was quantified by DCFH-DA with minor modification (Ye *et al*., 2018). The visceral organs from three zebrafish were pooled and homogenized in ice-cold phosphate buffer saline (pH 7.4) at a ratio of 1:15 (w/v). The homogenates were centrifuged to remove debris, and the supernatant was collected and mixed with 25 μmol 2′, 7′-Dichlorofluorescin diacetate solution (Sigma) for 30 min at 37°C in dark. Fluorescence of the samples was monitored at an excitation wavelength of 490 nm and an emission wavelength of 515 nm by a microplate reader (Varioskan LUX, Thermo Scientific). The results were analysed with Student's *t* test. $^{*}P < 0.05$; $^{**}P < 0.01$.

Activity of HK, PFK, PK, PDH, α-KGDH, SDH, MDH

The enzymatic activity detection of hexokinase (HK), 6-phosphofructokinase (PFK), pyruvate kinase (PK), pyruvate dehydrogenase (PDH), α-ketoglutarate dehydrogenase (α-KGDH), succinate dehydrogenase (SDH) and malic dehydrogenase (MDH) were measured by PMS (Phenazine methosulfate) method, slightly modified (Li *et al*., 2019). The visceral organs from three zebrafish were pooled and homogenized in ice-cold PBS (pH 7.4) were added at a ratio of 1:15 (w/v). The homogenates were centrifuged to remove debris, and supernatant was collected. Protein concentration was measured by Bradford method (Hammond and Kruger, 1988). The activity of HK, PFK and PK was measured using commercial kits (Jiancheng Corp., Nanjing, China). The reaction buffer for PDH and α-KGDH included 0.5 mM MTT, 1 mM $MgCl_2$, 6.5 mM PMS, 0.2 mM TPP, 50 mM PBS and 2 mM sodium pyruvate (for PDH) or 2 mM sodium α-Ketoglutaric acid (for α-KGDH). The reaction systems of SDH and MDH included 0.5 mM MTT, 6.5 mM PMS, 5 mM succinate, 50 mM PBS. All the reactions were performed in a final volume of 200 μl in 96-well plate. Subsequently, the plate was incubated at 37°C for 5 min for PDH, α-KGDH, SDH and MDH. The optical absorbance was performed in microplate reader (Varioskan LUX, Thermo Scientific) at 566 nm. The results were analysed with Student's *t* test. $^{*}P < 0.05$; $^{**}P < 0.01$.

Gene expression by quantitative real-time polymerase chain reaction (qRT-PCR)

The expression of genes was analysed by the qRT-PCR as described previously (Cheng *et al*., 2019). Total RNA was isolated from spleen pooled from three *D. rerio* with Trizol (Invitrogen, Carlsbad, CA, USA). qRT-PCR was performed in 384-well plates with a total volume of 10 μl containing 5 μl 2 × SYBR Premix Ex Taq™, 2.6 μl H_2O, 2 μl cDNA template and 0.2 μl each of forward and reverse primers (10 μM). The cycling parameters were listed as follows: 95°C for 30 s to activate the polymerase; 40 cycles of 95°C for 10 s; and 60°C for 30 s. Fluorescence measurements were performed at 72°C for 1 s during each cycle. Cycling was terminated at 95°C with a calefactive velocity of 5°C s^{-1} to obtain a melting curve. All qRT-PCR reactions were performed for three biological replicates, and the data

for each sample were expressed relative to the expression level of β-actin gene by $2^{-\Delta\Delta CT}$ method. Gene-specific primers used for qRT-PCR are shown in Table S4.

Determination of intracellular ATP and NADPH

Intracellular ATP was quantified by Cell Titer-Glo™ Luminescent Cell Viability kit according to the manufacturer's instruction (Promega, Madison, WI, USA) as previously described (Cheng *et al*., 2018b). Briefly, the visceral organs from three zebrafish were pooled and homogenized in ice-cold phosphate buffer saline (pH 7.4). After removing the debris after centrifugation, the supernatant was collected and mixed with Single-One-Step in equal volume in 96-well white plate. After incubation, the luminescence was read in a luminescent plate reader (Victor X5, PerkinElmer, Waltham, MA, USA). The results were analysed with Student's *t* test. $^{*}P < 0.05$; $^{**}P < 0.01$.

Quantification of NADPH was performed with Enzychrom™ $NADP^{+}$/NADPH assay kit according to manufacturer's instruction (BioAssay Systems, Hayward, CA, USA). The results were analysed with Student's *t* test. $^{*}P < 0.05$; $^{**}P < 0.01$.

Acknowledgements

This work was sponsored by grants from NSFC project (31822058, 31672656, 31872602), and the Fundamental Research Funds for the Central Universities (18lgzd14, 19lgyjs42).

Conflict of interests

The authors declare there is no conflict of interest.

Author contributions

BP conceptualized and designed the project. QYG, ZGC, LFY and MJ performed experiments. QYG, LFY, ZGC, MJ and MJY performed data analysis. BP, QYG, LFY and MJ interpreted the data. BP wrote the manuscript. All the authors reviewed the manuscript.

References

Aguirre-Guzman, G., Mejia Ruiz, H., and Ascencio, F. (2004) A review of extracellular virulence product of Vibrio species important in diseases of cultivated shrimp. *Aquacult Res* **35:** 1395–1404.

Balebon, M.C., Andreu, M.J., Bordas, M.A., Zorrila, I., Morinigo, M.A., and Borrego, J.J. (1998a) Pathogenicity of *Vibrio alginolyticus* for culture gilt-head sea bream (*Sparus aurata* L.). *Appl Envrion Microbiol* **64:** 4269–4275.

Balebona, M.C., Zorrilla, I., Morinigo, M.A., and Borrego, J.J. (1998b) Survey of bacterial pathologies affecting farmed gilt-head sear bream (*Sparus aurata* L.) in southwestern Spain from 1990 to 1996. *Aquaculture* **166:** 19–35.

Cervenka, I., Agudelo, L.Z., and Ruas, J.L. (2017) Kynurenines. Tryptophan's metabolites in exercise, inflammation, and mental health. *Science* **357:** eaaf9794.

Chen, Y., and Guillemin, G.J. (2009) Kynurenine pathway metabolites in humans: disease and healthy states. *Int J Tryptophan Res* **2:** 1–19.

Chen, X.H., Zhang, B.W., Li, H., and Peng, X.X. (2015) Myo-inositol improves the host' s ability to eliminate balofloxacin-resistant *Escherichia coli*. *Sci Rep* **5:** 10720.

Chen, X.H., Liu, S.R., Peng, B., Li, D., Cheng, Z.X., Zhu, J.X., *et al*. (2017) Exogenous L-valine promotes phagocytosis to kill multidrug-resistant bacterial pathogens. *Front Immunol* **8:** 207.

Cheng, Z.X., Ma, Y.M., Li, H., and Peng, X.X. (2014) N-acetylglucosamine enhances survival ability of tilapias infected by *Streptococcus iniae*. *Fish Shellfish Immunol* **40:** 524–30.

Cheng, Z.X., Chu, X., Wang, S.N., Peng, X.X., and Li, H. (2018) Six genes of *ompA* family shuffling for development of polyvalent vaccines against *Vibrio alginolyticus* and *Edwardsiella tarda*. *Fish Shellfish Immunol* **75:** 308–315.

Cheng, Z.X., Yang, M.J., Peng, B., Peng, X.X., Lin, X.M., and Li, H. (2018) The depressing central carbon and energy metabolisms mediate levofloxacin resistance in *Vibrio alginolyticus*. *J Proteomics* **181:** 83–91.

Cheng, Z.X., Guo, C., Chen, Z.G., Yang, T.C., Zhang, J.Y., Wang, J., *et al*. (2019) Glycine, serine and threonine metabolism confounds efficacy of complement-mediated killing. *Nat Commun* **10:** 3325.

Cook, D.W., O'Leary, P., Hunsucker, J.C., Sloan, E.M., Bowers, J.C., Blodgett, R.J., *et al*. (2002) *Vibrio vulnificus* and *Vibrio parahaemolyticus* in US retail shell oysters: a national survey from June 1998 to July 1999. *J Food Prot* **65:** 79–87.

Di Pinto, A., Ciccarese, G., Tantillo, G., Catalano, D., and Forte, V.T. (2005) A collagenase-targeted multiplex PCR assay for identification of *Vibrio alginolyticus*, *Vibrio cholerae*, and *Vibrio parahaemolyticus*. *J Food Prot* **68:** 150–153.

Dubreil, E., Gautier, S., Fourmond, M.P., Bessiral, M., Gaugain, M., Verdon, E., and Pessel, D. (2017) Validation approach for a fast and simple targeted screening method for 75 antibiotics in meat and aquaculture products using LC-MS/MS. *Food Addit Contam Part A Chem Anal Control Expo Risk Assess* **34:** 453–468.

Dukes, A., Davis, C., Refaey, E.M., Upadhyay, S., Mork, S., Arounleut, P., *et al*. (2015) The aromatic amino acid tryptophan stimulates skeletal muscle IGF1/p70s6k/mTor signaling in vivo and the expression of myogenic genes in vitro. *Nutrition* **31:** 1018–1024.

Düvel, K., Yecies, J.L., Menon, S., Raman, P., Lipovsky, A.I., Souza, A.L., *et al*. (2010) Activation of a metabolic gene regulatory network downstream of mTOR complex 1. *Mol Cell* **39:** 171–183.

Fernstrom, J.D. (2016) A perspective on the safety of supplemental tryptophan based on its metabolic fates. *J Nutr* **146:** 2601S–2608S.

Fu, K., Li, J., Wang, Y., Liu, J., Yan, H., Shi, L., and Zhou, L. (2016) An innovative method for rapid identification and detection of *Vibrio alginolyticus* in different infection models. *Front Microbiol* **7:** 651.

Ganeshan, K., and Chawla, A. (2014) Metabolic regulation of immune responses. *Annu Rev Immunol* **32:** 609–634.

Gong, Y., Zhai, G., Su, J., Yang, B., Jin, J., Liu, H., *et al*. (2018) Different roles of insulin receptor a and b in maintaining blood glucose homeostasis in zebrafish. *Gen Comp Endocrinol* **269:** 33–45.

Groer, M.W., Yolken, R.H., Xiao, J.C., Beckstead, J.W., Fuchs, D., Mohapatra, S.S., *et al*. (2011) Prenatal depression and anxiety in toxoplasma gondii-positive women. *Am J Obstet Gynecol* **204:** 433.e1–433.e7.

Gu, D., Guo, M., Yang, M.J., Zhang, Y.X., Zhou, X.H., and Wang, Q.Y. (2016) A sigma E-mediated temperature gauge controls a switch from LuxR-mediated virulence gene expression to thermal stress adaptation in *Vibrio alginolyticus*. *PLos Pathog* **12:** e1005645.

Guo, C., Huang, X.Y., Yang, M.J., Wang, S., Ren, S.T., Li, H., *et al*. (2014) GC/MS-based metabolomics approach to identify biomarkers differentiating survivals from death in crucian carps infected by *Edwardsiella tarda*. *Fish Shellfish Immunol* **39:** 215–222.

Hammond, J., and Kruger, N. (1988) The Bradford method for protein quantitation. *Methods Mol Biol* **32:** 9–15.

Huttunen, R., Syrjänen, J., Aittoniemi, J., Oja, S.S., Raitala, A., Laine, J., *et al*. (2010) High activity of indoleamine 2,3-dioxygenase enzyme predicts disease severity and case fatality in bacteremic patients. *Shock* **33:** 149–154.

Ispasanie, E., Micoli, F., Lamelas, A., Keller, D., Berti, F., De Riccio, R., *et al*. (2018) Spontaneous point mutations in the capsule synthesis locus leading to structural and functional changes of the capsule in serogroup A meningococcal populations. *Virulence* **9:** 1138–1149.

Jiang, M., Gong, Q.Y., Lai, S.S., Cheng, Z.X., Chen, Z.G., Zheng, J., and Peng, B. (2018) Phenylalanine enhances innate immune response to clear ceftazidime-resistant *Vibrio alginolyticus* in *Danio rerio*. *Fish Shellfish Immunol* **84:** 912–919.

Jiang, M., Chen, Z.G., Zheng, J., and Peng, B. (2019) Metabolites-enabled survival of Crucian Carps infected by *Edwardsiella tarda* in high water temperature. *Front Immunol* **10:** 1991.

Kang, C.H., Shin, Y., Jang, S., Jung, Y., and So, J.S. (2016) Antimicrobial susceptibility of *Vibrio alginolyticus* isolated from oyster in Korea. *Environ Sci Pollut Res Int* **23:** 21106–21112.

Karami, A., Christianus, A., Ishak, Z., Arif Syed, M., and Charles Courteney, C. (2011) The effects of intramuscular and intraperitoneal injections of benzo[a]pyrene on selected biomarkers in *Clarias gariepinus*. *Ecotoxicol Environ Saf* **74:** 1558–1566.

Lee, J.K., Jung, D.W., and Eom, S.Y. (2008) Occurrence of *Vibrio parahaemolyticus* in oysters from Korean retail outlets. *Food Control* **19:** 990–994.

Li, L., Wang, S., Zhang, H., Xi, L., Zhang, J., Zhang, X., *et al*. (2018) Development and evaluation of in murine model, of an improved live-vaccine candidate against brucellosis from to *Brucella melitensis* vjbR deletion mutant. *Microb Pathog* **124:** 250–257.

Li, Z., Wang, Y., Li, X., Lin, Z., Lin, Y., Srinivasan, R., *et al*. (2019) The characteristics of antibiotic resistance and phenotype in 29 outer-membrane protein mutant strains in *Aeromonas hydrophila*. *Environ Microbiol* **21:** 4614–4628.

Ma, Y.M., Yang, M.J., Wang, S., Li, H., and Peng, X.X. (2015) Liver functional metabolomics discloses an action of L-leucine against *Streptococcus iniae* infection in tilapias. *Fish Shellfish Immunol* **45:** 414–421.

Manjusha, S., Sarita, G.B., Elyas, K.K., and Chandrasekaran, M. (2005) Multiple antibiotic resistances of *Vibrio* isolated from coastal and brackish water areas. *Am J Biochem Biotechnol* **1:** 201–206.

Moffett, J.R., and Namboodiri, M.A. (2003) Tryptophan and the immune response. *Immunol Cell Biol* **81:** 247–265.

Moffett, J.R., Blinder, K.L., Venkateshan, C.N., and Namboodiri, M.A.A. (1998) Differential effects of kynurenine and tryptophan treatment on quinolinate immunoreactivity in rat lymphoid and non-lymphoid organs. *Cell Tissue Res* **293:** 525–524.

Oh, E.G., Son, K.T., Yu, H., Lee, T.S., Lee, H.J., Shin, S.B., *et al*. (2011) Antimicrobial resistance of *Vibrio parahaemolyticus* and *Vibrio alginolyticus* strains isolated from farmed fish in Korea from 2005 through 2007. *J Food Prot* **74:** 380–6.

Peng, B., Su, Y.B., Li, H., Han, Y., Guo, C., Tian, Y.M., and Peng, X.X. (2015) Exogenous alanine or/and glucose plus kanamycin kills antibiotic-resistant bacteria. *Cell Metab* **21:** 249–261.

Peng, B., Ma, Y.M., Zhang, J.Y., and Li, H. (2015) Metabolome strategy against *Edwardsiella tarda* infection through glucose-enhanced metabolic modulation in tilapias. *Fish Shellfish Immunol* **45:** 869–876.

Peng, B., Li, H., and Peng, X.X. (2015) Functional metabolomics: from biomarker discovery to metabolome reprogramming. *Protein Cell* **6:** 628–637.

Reilly, G.D., Reilly, C.A., and Smith, E.G. (2011) Baker-Austin C. *Vibrio alginolyticus*-associated wound infection acquired in British waters, Guernsey, July. *Euro Surveill* **16:** 19994.

Sas, K., Szabó, E., and Mitochondria, Vécsei L. (2018) Oxidative stress and the Kynurenine system, with a focus on ageing and neuroprotection. *Molecules* **23:** E191.

Su, Y.B., Peng, B., Han, Y., Li, H., and Peng, X.X. (2015) Fructose restores susceptibility of multidrug-resistant *Edwardsiella tarda* to kanamycin. *J Proteome Res* **14:** 1612–1620.

Su, Y.B., Peng, B., Li, H., Cheng, Z.X., Zhang, T.T., Zhu, J.X., *et al*. (2018) Pyruvate cycle increases aminoglycoside efficacy and provides respiratory energy in bacteria. *Proc Natl Acad Sci USA* **115:** E1578–E1587.

Wen, X., Cui, L., Morrisroe, S., Maberry, D. Jr, Emlet, D., Watkins, S., *et al*. (2018) A zebrafish model of infection-associated acute kidney injury. *Am J Physiol Renal Physiol* **315:** F291–F299.

Yang, D., Elner, S.G., Bian, Z.M., Till, G.O., Petty, H.R., and Elner, V.M. (2007) Pro-inflammatory cytokines increase reactive oxygen species through mitochondria and NADPH oxidase in cultured RPE cells. *Exp Eye Res* **85:** 462–472.

Yang, M.J., Cheng, Z.X., Jiang, M., Zeng, Z.H., Peng, B., Peng, X.X., and Li, H. (2018) Boosted TCA cycle enhances survival of zebrafish to *Vibrio alginolyticus* infection. *Virulence* **9:** 634–644.

Yang, J., Zeng, Z.H., Yang, M.J., Cheng, Z.X., Peng, X.X., and Li, H. (2018) NaCl promotes antibiotic resistance by reducing redox states in *Vibrio alginolyticus*. *Environ Microbiol* **20:** 4022–4036.

Ye, J.Z., Su, Y.B., Lin, X.M., Lai, S.S., Li, W.X., Ali, F., *et al*. (2018) Alanine enhances aminoglycosides-induced ROS production as revealed by proteomic analysis. *Front Microbiol* **9:** 29.

Zeng, Z.H., Du, C.C., Liu, S.R., Li, H., Peng, X.X., and Peng, B. (2017) Glucose enhances tilapia against *Edwardsiella tarda* infection through metabolome reprogramming. *Fish Shellfish Immunol* **61:** 34–43.

Zhao, F., Zhou, D., Cao, H., Ma, L., and Jiang, Y. (2011) Distribution, serological and molecular characterization of *Vibrio parahaemolyticus* from shellfish in the eastern coast of China. *Food Control* **22:** 1095–1100.

Zhao, X.L., Wu, C.W., Peng, X.X., and Li, H. (2014) Interferon-α2b against microbes through promoting biosynthesis of unsaturated fatty acids. *J Proteome Res* **13:** 4155–4163.

Zhao, X.L., Han, Y., Ren, S.T., Ma, Y.M., Li, H., and Peng, X.X. (2015) L-proline increases survival of tilapias infected by *Streptococcus agalactiae* in higher water temperature. *Fish Shellfish Immunol* **44:** 33–42.

Supporting information

Additional supporting information may be found online in the Supporting Information section at the end of the article.

Table S1. Folds of change of metabolites of dying and survival groups compared to control.

Table S2. The sensitivity/specificity for the selected metabolites in predicting the survival of the animals.

Table S3. Folds of change of the crucial metabolites after tryptophan injection

Table S4. Primers for qRT-PCR

Fig. S1. Determination of LD50 of *V. alginolyticus* to *D. reiro*. A total of 210 individual zebrafish were randomly divided into 7 groups. They were injected with either 5 μl saline (0.85% sodium chloride) or 5 μl *V. alginolyticus* (4.0×10^7 CFU ml^{-1}, 8.0×10^7 CFU ml^{-1}, 1.2×10^8 CFU ml^{-1}, 1.6×10^8 CFU ml^{-1}, 2.0×10^8 CFU ml^{-1} or 2.4×10^8 CFU ml^{-1}) at the indicated concentration shown above. The death of fish was monitored for a total of 14 days post-infection. As we found that no fish died after 7 days post-infection, we used 7 days as the cut-off time-point to monitor fish death in the following study. The dose that causes 50% of death is considered as LD_{50}.

Fig. S2. ROC curves of the biomarker results from Survival group vs. Dying group. ROC, receiver operating characteristics; AUC, area under the curve.

Fig. S3. Metabolomic analysis of saline- and tryptophan-treated *D. rerio*. A total of 40 zebrafish were randomly divided into control and experimental groups with 20 zebrafish for each group. Twenty individual zebrafish were in each tank. These animals were injected individually with 5 μl 50 mM tryptophan by intraperitoneal injection, and treated with the same volume of sterile saline as control. Both two groups were injected once daily for 6 days, after the last administration, 10 zebrafish from each group was collected for their body fluids for GC-MS analysis. (A) Heat map showing relative abundance of metabolites (Wilcoxon $P < 0.01$) in control and tryptophan group. Heat map scale (blue to yellow: low to high abundance) is shown at bottom. (B) Z scores (standard deviation from average) corresponding to data in (A). (C) Principle component analysis of control *and* tryptophan group. Each dot represents one technical replicate. (D) The distribution of differential abundance of metabolites' weight from method of OPLS-DA to control and experimental samples. Triangle represents metabolites and candidate biomarkers are highlighted with red. (E) Folds of change of the metabolites.

